Comparative Study of Carbon and BN Nanographenes: Ground Electronic States and Energy Gap Engineering

Xingfa Gao,[†] Zhen Zhou,[‡] Yuliang Zhao,[§,||] Shigeru Nagase,*[,†] S. B. Zhang,[⊥] and Zhongfang Chen*[,⊥,#]

Department of Theoretical and Computational Molecular Science, Institute for Molecular Science, Myodaiji, Okazaki 444-8585, Japan, Institute of New Energy Material Chemistry, Institute of Scientific Computing, Nankai University, Tianjin 300071, China, Laboratory for Bio-Environmental Effects of Nanomaterials and Nanosafety, Institute of High Energy Physics, Chinese Academy of Sciences, Beijing 100049, China, National Center for Nanoscience and Technology of China, Beijing 100080, China, Department of Physics, Applied Physics, and Astronomy, Rensselaer Polytechnic Institute, Troy, New York 12180, and Department of Chemistry, Institute for Functional Nanomaterials, University of Puerto Rico, San Juan, PR 00931

Received: February 21, 2008; Revised Manuscript Received: May 14, 2008

The relationship between stabilities and shape configurations of carbon and boron nitride (BN) nanographenes (NGs) was studied at the B3LYP/6-31G* level of theory. The HOMO−LUMO energy gaps of rectangular-shaped carbon nanographenes (CNGs) decrease as the graphene sizes increase with a direct inverse dependence on the length of zigzag edge. Due to the double zigzag edge boundaries, the CNGs with long zigzag edges have open-shell singlet ground states; in contrast, the HOMO−LUMO energy gaps of BN nanographenes (BNNGs) have a weak dependence with size; all BNNGs have closed-shell singlet ground states, and those with long zigzag edges have slightly larger energy gaps. CNGs with long zigzag edges are less favorable energetically than their structural isomers with long armchair edges, while the BNNGs have the opposite preference. Chemical modifications that change the long zigzag edge into armchair type can efficiently stabilize the kinetically unstable CNGs (with open-shell singlet ground states) and modify their energy gaps.

1. Introduction

Graphene,[1] an atomic monolayer of carbon atoms arranged in a honeycomb lattice, has rather a unique electronic structure.[2–10] This results in many fascinating phenomena such as the anomalously quantized Hall effects,[11–16] massless quantum particles,[17,18] and electric field effect,[19] which endows graphene great potential as the new generation of carbon electronics;[1,20] electronic devices with exciting functions based on graphene, such as field-effect transistors[21–23] and solid-state gas sensors,[24] have been proposed.

The lack of an energy gap in graphene's electronic spectra is one of the biggest obstacles that prevent using graphene in carbon electronics, for example as transistors;[25–27] thus, it is highly important to effectively engineer its band gap. It has been shown that the energy gaps of patterned graphene nanoribbons can be tuned by fabricating their widths,[27] and that the graphene–substrate interaction can also lead to a band gap opening in epitaxial graphene.[25,26]

Previous computational investigations show that zigzag-edged carbon graphene nanoribbons,[6,28–32] and rectangular nanographenes (NGs) with more than four benzene rings at the zigzag edges[3] have open-shell singlet ground states, and it is the existence of the zigzag edges that determines the electronic structures of these carbon nanographenes (CNGs). The boron nitride nanographene (BNNG) monolayer was also prepared,[33] and the structural and electronic properties of BNNG were studied theoretically.[34]However, many questions are still pending: with zigzag edges, do BNNGs also have open-shell singlet ground states as carbon graphenes? Since the radical character makes the open-shell singlets of CNGs highly reactive, is it possible to stabilize them in some way and tune their energy gaps at the same time? In this paper, we present more systematic studies on the rectangular CNGs and their BN analogues and propose some chemical modification approaches to efficiently stabilize unstable graphenes.

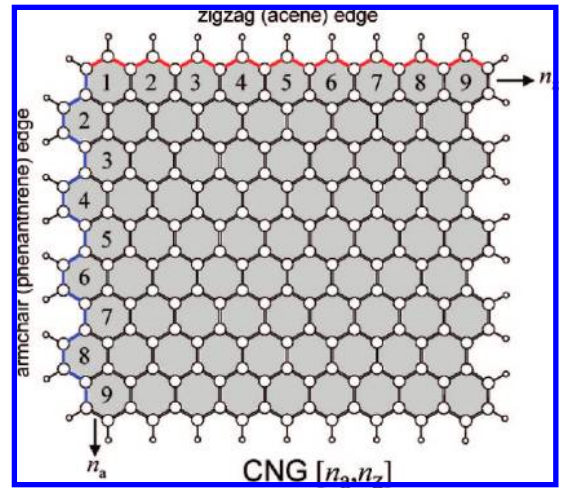

Figure 1. Rectangular shaped graphene (CNG) with zigzag and armchair edges.

* To whom correspondence should be addressed. E-mail: (S.N.) nagase@ims.ac.jp; (Z.C.) chenz4@rpi.edu.
† Institute for Molecular Science.
‡ Nankai University.
§ Chinese Academy of Sciences.
|| National Center for Nanoscience and Technology of China.
⊥ Rensselaer Polytechnic Institute.
University of Puerto Rico.

10.1021/jp801679j CCC: $40.75
Published on Web 07/19/2008

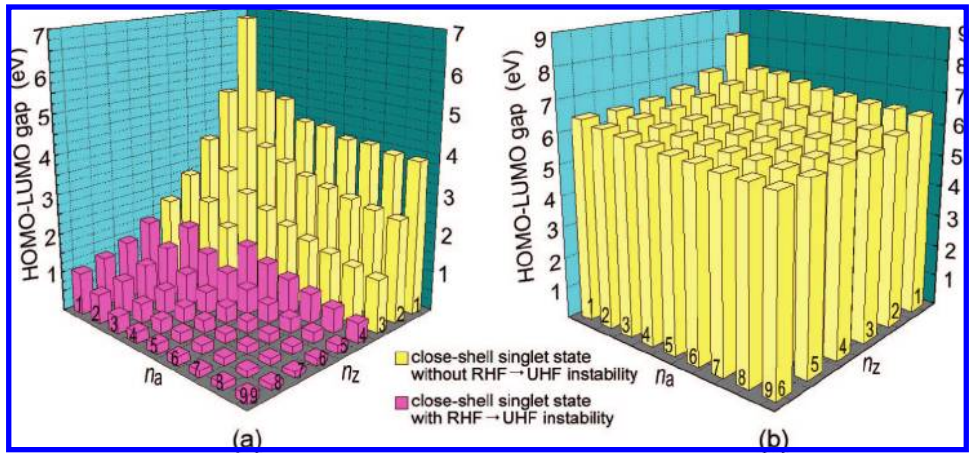

Figure 2. HOMO−LUMO gaps of CNGs (a) and BNNGs (b) at the lowest-energy closed-shell singlet states (RB3LYP/6-31G*//RB3LYP/6-31G*). n_a and n_z are the numbers of fused benzene rings contained in the armchair and zigzag edges of the model. The species with closed-shell singlet ground states and open-shell singlet ground states are represented by yellow and pink bars, respectively.

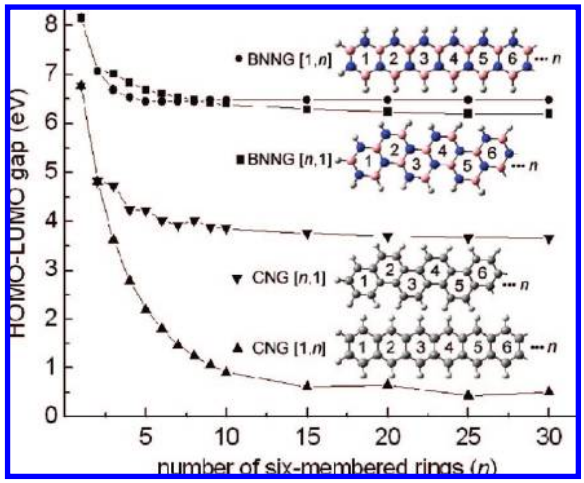

Figure 3. HOMO−LUMO gaps of CNG and BNNG stripes (RB3LYP/6-31G*//RB3LYP/6-31G*, nitrogen atoms in dark gray).

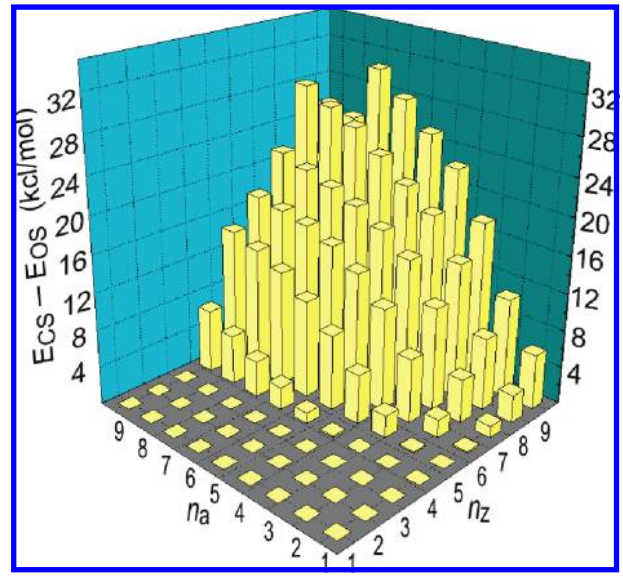

Figure 4. The normalized energy difference between closed-shell singlet and open-shell singlet states of CNGs.

2. Computational Method

Initially the closed-shell singlets of the CNG and BNNG models were optimized with spin-restricted Kohn−Sham (RKS) method, using the hybrid B3LYP exchange and correlation functionals combined with the 6-31G* basis set (RB3LYP/6-31G*). Then, based on these optimized structures, the open-shell singlets were computed using unrestricted broken spin-symmetry wave function (UBS-B3LYP/6-31G*//RB3LYP/6-31G*), while the triplet states were calculated with unrestricted density functional computations (UB3LYP/6-31G*//RB3LYP/6-31G*). This approach is a balance of accuracy and CPU cost, since the geometries of the open-shell singlets and triplets fully optimized using the unrestricted DFT are very closed to the closed-shell singlets. The symmetries of CNGs were constrained to C_{2H} or C_{2v} and those of BNNGs were constrained to C_s in all of the above computations. All calculations were performed using Gaussian 03 package.[35]

Since armchair and zigzag are the two elemental geometrical shapes for CNG and BNNG edges from which other hybrid shapes can be derived, rectangular-shaped graphenes and BNNGs with pure armchair or zigzag edges were intensively studied. Such a graphene model is exemplified in Figure 1, where the dangling bonds of peripheral carbons are saturated with hydrogens. This model is referred to as a nanographene in this work. We used the numbers of benzenoid units contained in the armchair and zigzag edges, as written as CNG $[n_a,n_z]$, as the unique notation for a CNG. On the basis of its topology, the molecular formula of a CNG $[n_a,n_z]$ is C_xH_y, where x and y are given by eqs 1 and 2.

$$x = 2(n_a n_z + n_a + n_z) \quad (1)$$

$$y = 2(n_a + n_z + 1) \quad (2)$$

A BNNG model was constructed by replacing each C−C bond of a CNG $[m,n]$ with a B−N bond, and the obtained BNNG is labeled as BNNG $[m,n]$. The molecular formula for a BNNG is $B_zN_zH_y$, where $z = x/2$. From the molecular equations, one can see that CNGs $[m,n]$ and $[n,m]$ have the same molecular formula and form an isomeric pair; the same fact is also for BNNGs $[m,n]$ and $[n,m]$.

3. Results and Discussion

3.1. The Open-Shell Singlet Ground States of CNGs with Long Zigzag Edges. Figure 2a shows the HOMO−LUMO energy gaps of the CNGs calculated at closed-shell singlet states

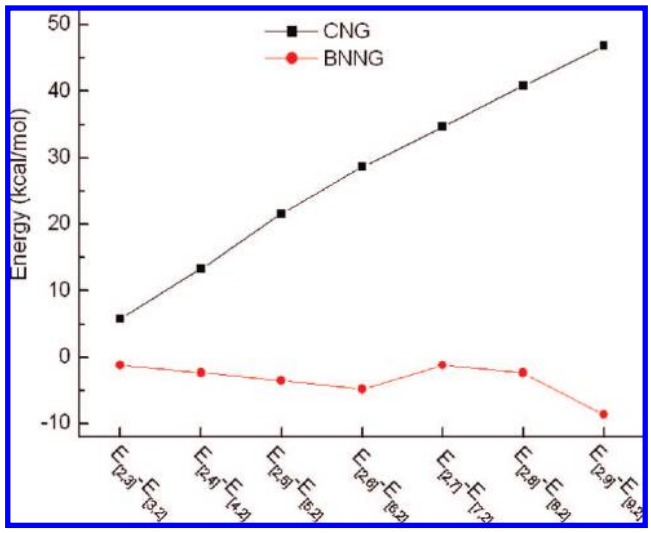

Figure 5. Energy difference of isomeric CNGs and BNNGs.

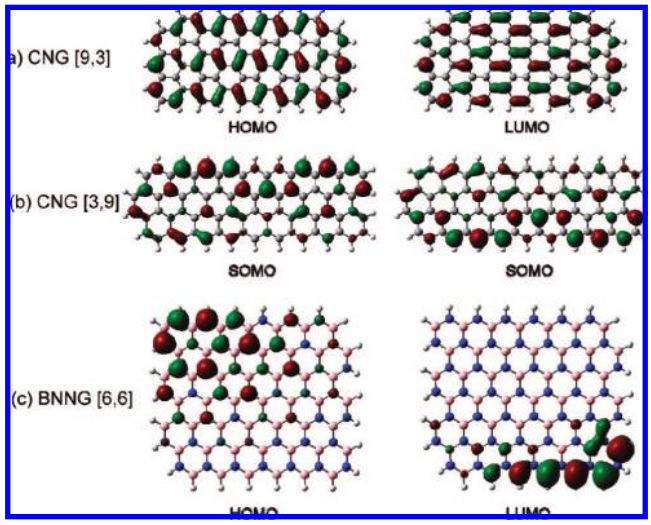

Figure 6. Frontier molecular orbitals (B3LYP/6−31G*) computed at the ground states: closed-shell singlet for CNG [9,3] and BNNG [6,6]; open-shell singlet for CNG [3,9].

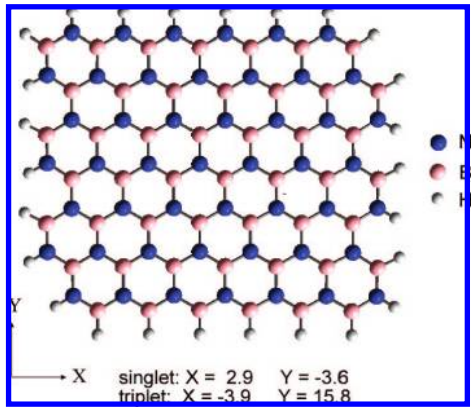

Figure 7. Dipole moments (Debye) of BNNG [6,6] at singlet and triplet states.

with the spin-restricted Kohn−Sham (RKS) B3LYP/6-31G* method. The energy gap decreases with increasing both n_a and n_z, indicating a decreasing kinetic stability as the total number of benzenoid rings contained in CNGs increases (see Figure 2a). The inverse dependence of gap on n_z, however, is remarkably stronger than that on n_a, as shown in Figure 2a and more explicitly in Figure 3, where the energy gaps of the extreme cases CNGs [n,1] and [1,n] are plotted. CNGs [n,1] and [1,n] are known as polyphenanthrene and polyacene, whose electronic structures and stabilities have stimulated great research interest.[30,32,36,37] The gap of CNG [1,n] reduces from 6.8 to below 1.0 eV rapidly as n increases from 1 to 10; contrarily, CNG [n,1] has a much slower decreasing tendency (see Figure 3). Similar large inverse-dependence of HOMO−LUMO energy gaps with the length of zigzag-edge has been predicted for anomalously shaped polycyclic aromatic hydrocarbons (PAHs).[38–46]

The small HOMO−LUMO gap of a large CNG hints that a single-determinant wave function might no longer describe appropriately the ground-state of the CNG and that other types of wave functions might have lower energies. Indeed, recent calculations for a polyacene,[30,36] cycloacene, or zigzag carbon nanotube[47] have shown that the energies of the open-shell singlet (E_{OS}) and triplet (E_T) become lower in energy than the corresponding closed-shell singlet (E_{CS}) when the system contains enough long zigzag edges. Figure 2a illustrates whether the RKS solution is the ground-state for a CNG: all CNGs with $n_z \leq 3$ have closed-shell singlet ground states as shown as the yellow bars; however, all those with $n_z \geq 6$ have open-shell singlet ground states as shown as the pink bars; the ground states of those with $n_z = 4$, 5, and 6 are determined by the values of both n_a and n_z. Figure 4 plots the normalized energy difference of E_{CS} and E_{OS} (energy difference divided by the number of benzene rings) which shows ($E_{CS} - E_{OS}$) increases as the size of CNG increases. These results suggest that, among the computationally economic single-determinant wave function methods, using a UBS ansatz is essential to properly calculate the ground-state properties for a large CNG. The values of ($E_{CS} - E_{OS}$) as well as those of $<S^2>$ and ($E_T - E_{OS}$) are given in Table S1 in the Supporting Information.

The relative energies of some isomeric CNGs are plotted in Figure 5 (see Table S2 in Supporting Information for energy data), which suggest that CNGs with a longer zigzag edge have a lower thermodynamic stability than their structural isomers with a long armchair edge. For example, CNG [2,9] has a higher energy than CNG [9,2] by 46.8 kcal/mol. Similar relative stabilities have been predicted for graphene ribbons without hydrogen-termination.[48] This phenomenon can be interpreted with the fact that the outmost carbons in an armchair edge are in pairs, sharing the extra stabilization by forming "double bonds" and contrarily that the outmost carbons in a zigzag edge are discrete with radical character.[31,49]

3.2. The Closed-Shell Singlet Ground States of BNNGs. BNNGs have different features as compared to CNGs. BNNGs have only a weak dependence of stability on their edge shapes and lengths. As shown in Figure 2b, the decrease of HOMO−LUMO gaps caused by the increase of BNNG sizes is much slower than that for CNGs (Figure 2a); all BNNGs have closed-shell singlet ground electronic states. As illustrated in Figure 3, both BNNGs [1,n] and [n,1] keep large energy gaps of about 6 eV when n reaches 30. This implies that even larger BNNGs are semiconductive, in accordance with the well-known fact that BN nanotubes are all semiconductors.[50,51]

A BNNG with a longer zigzag edge (BNNG [m,n], $n > m$) has a relatively larger kinetic stability (see HOMO−LUMO gaps in Figure 2b and Figure 3) and thermodynamic stability (see Figure 5 and Table S3 in Supporting Information) than its structural isomer (BNNG [n,m]) that has a longer armchair edge; this is opposite to the case of CNG where a longer zigzag is kinetically and thermally disfavored.

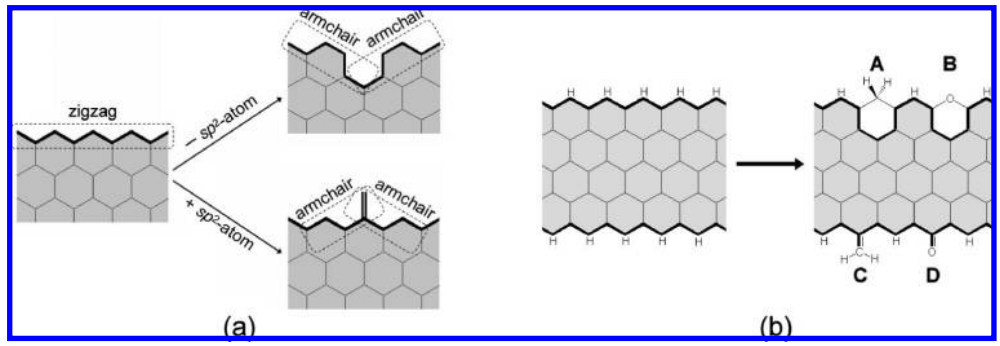

Figure 8. (a) Splitting the long zigzag-type edge into two short armchair-type by removing a sp^2-atom and adding a sp^2-atom. (b) Chemical modifications A−D that alter the edges from zigzag (left) to armchair (right) type.

CHART 1: CNG [4,9] and Its Derivative Structures Together with Their HOMO-LUMO Energy Gaps (RB3LYP/6-31G*)

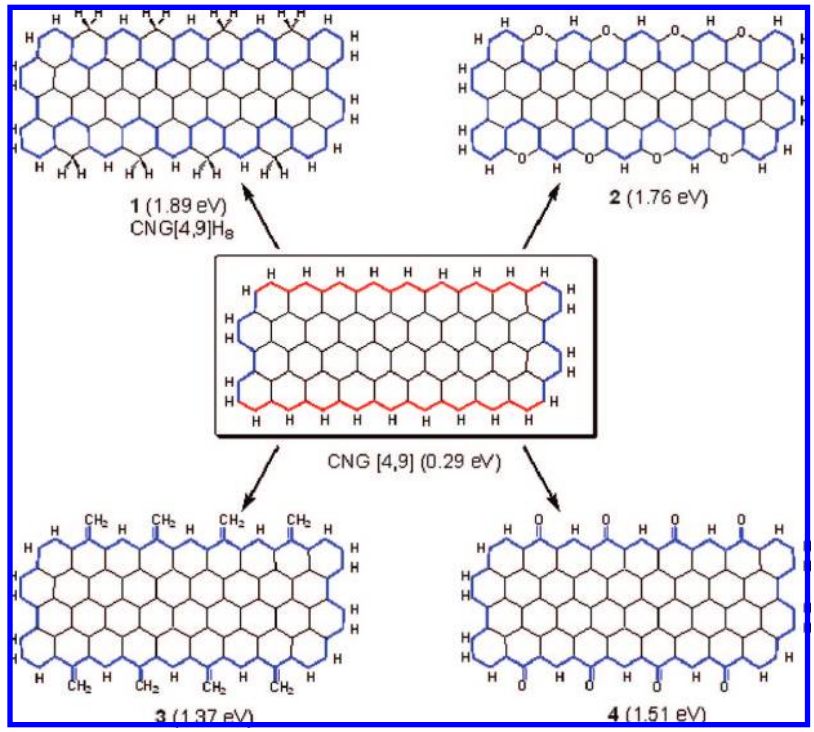

3.3. The Frontier Molecular Orbitals of CNGs and BNNGs. The frontier molecular orbitals of CNG [9,3], CNG [3,9] and BNNG [6,6] are shown in Figure 6 as examples. Unlike the CNG[9,3] closed-shell singlet ground-state whose HOMO and LUMO are distributed somewhat evenly in the entire molecular plane (Figure 6a), the SOMOs of the CNG[3,9] open-shell singlet are distributed mainly along the two zigzag edges (Figure 6b). The located spin state at the zigzag edge has been reported in the previous studies.[3–7,52] BNNG [6,6] has a closed-shell ground state; its HOMO and LUMO are also distributed separated along the two zigzag edges (Figure 6c); HOMO is mainly located at the outermost nitrogens in one zigzag edge while LUMO at the outermost borons in another zigzag edge. Therefore, it could be expected that an intermolecular charge movement takes place between the zigzag edges upon excitation of BNNG [6,6]. This was demonstrated by our B3LYP/6−31G* calculations, which showed that the dipole moment in the Y direction changes significantly during the excitation of BNNG [6,6] from ground (singlet) state to the lowest-energy triplet state (Figure 7). The different electronic structures of CNGs and BNNGs are due to their different atomic constituents and electron distributions. In a large CNG, electronic charge density is distributed homogenously in the carbon framework, which leads to a large number of near-degenerate states.[36,53] However, because the electronegativity of N (e_N = 3.04) is large than that of B (e_N = 2.04),[54] in a BNNG, the electronic charge density distribution in the framework of BNNG is strongly asymmetric (see Figure S1 in Supporting Information). As a result, the HOMO−LUMO gap of a CNG diminishes to nearly zero while that of a BNNG remains large and independent with the molecular size.

3.4. Transferring the Open-Shell CNG Singlet States to Kinetically Stable Structures by Chemical Modifications. Since zigzag edges are the labile sites that cause instability, one may expect that an unstable CNG with long zigzag edges would become stable after most of the zigzag edges being changed into armchair type. Figure 8a illustrates two ways that transfer a long zigzag edge into armchair type, and Figure 8b exemplifies four chemical modifications (**A**−**D**) that realize such a transformation. To check whether these region-selective reactions enhance the stability of CNG [4,9], **1**−**4** (see Chart 1) that were derived from CNG [4,9] were calculated. We first optimized the geometries of **1**−**4** with the RB3LYP/6-31G* method and then examined the stabilities of the obtained wave

CHART 2: Hydrides of CNG [4,9][a]

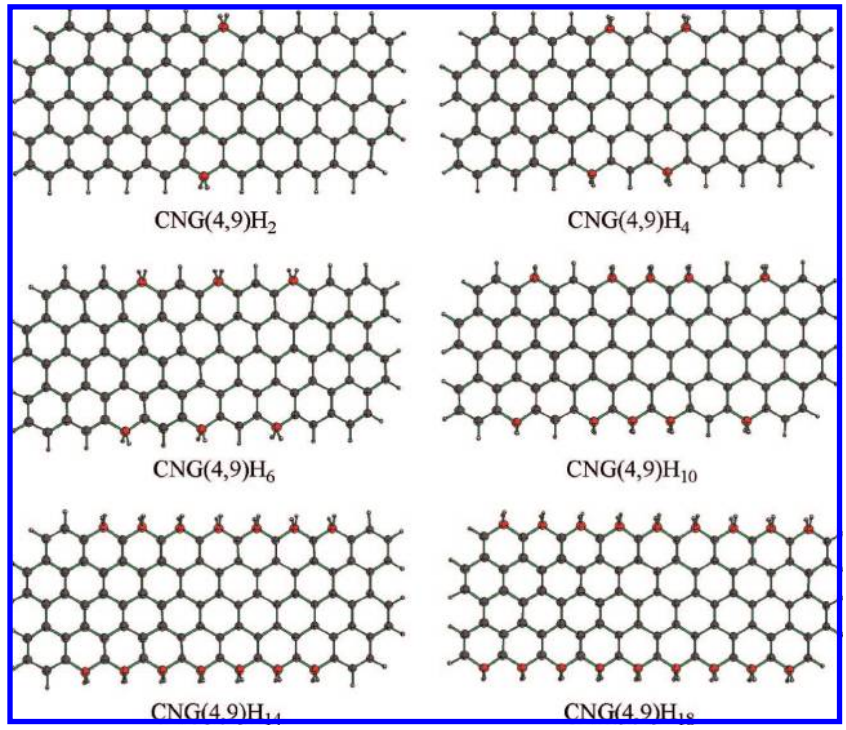

[a] The sp^3 carbon atoms are highlighted in red.

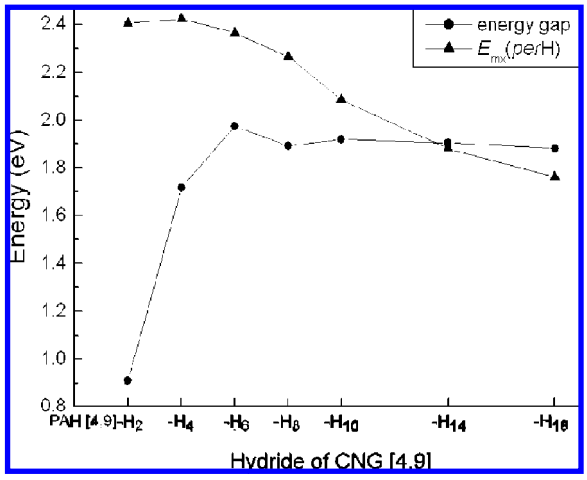

Figure 9. Reaction energies and HOMO−LUMO energy gaps of hydrogenated CNGs with respect to the extent of hydrogenation.

functions by using the "stable" keyword in Gaussian 03.[35] The RB3LYP HOMO−LUMO gaps have been labeled in Chart 1. After modifications, the gap of the pristine CNG [4,9] is enhanced from 0.29 eV to above 1.37 eV (see Chart 1). Contrasting to CNG [4,9] whose closed-shell singlet has a RHF → UHF instability and is inferior to the open-shell singlet by 23.21 kcal/mol (see Figure 4 and Table S1 in Supporting Information), **1**−**4** all have closed-shell ground-state electronic structures. These results show that chemical modifications **A**−**D** efficiently stabilize kinetically unstable CNGs. Comparing the gaps of **1**−**4** (see Chart 1), it is clear that **A** and **B** are superior to **C** and **D** in stabilizing CNG [4,9]. Because **A** and **B** reduce the total numbers of sp^2-carbons in the aromatic surfaces while **C** and **D** increase the total numbers of sp^2-carbons, the superiority of **A**, **B** to **C**, **D** is consistent with our previous result that a larger aromatic surface leads to a smaller HOMO−LUMO gap.

We further studied the stabilizing efficiency of **A** (i.e., hydrogenation). Equations 3 and 4 define the average hydrogenation energy $E_{rxn}(perH)$ for the hydrogenation of CNG.

$$\mathrm{CNG}[n_a, n_z] + n\mathrm{H} = \mathrm{CNG}[n_a, n_z]\mathrm{H}_n + E \quad (3)$$

$$E_{rxn}(perH) = E/n \quad (4)$$

We calculated the average hydrogenation energy $E_{rxn}(perH)$ and HOMO−LUMO gap for six hydrides of CNG [4,9] (see Chart 2) in addition to **1** of Chart 1. The results are plotted in Figure 9. Both $E_{rxn}(perH)$ and energy gap have a maximum point as the number of attached hydrogens increases. $E_{rxn}(perH)$ reaches its maximum at CNG [4,9]H_4 and then keeps reducing; however, the energy gap reaches the maximum at CNG [4,9]H_6 and then becomes a constant (see Figure 9). The decreasing dependence of $E_{rxn}(perH)$ with respect to the hydrogenation extent has also been found for zigzag-edged graphene nanoribbons.[29] Four to approximately six is the most appropriate hydrogenation number for CNG [4,9], which yield the hydrides with the largest kinetic stability and strongest C−H bond. These results give important indication about stabilizing a graphene structure and controlling its energy gap. Because of the higher reactivity of the zigzag sites, these region-selective reactions might be readily experimentally realized and thus have potentials in applications. Very recently, Kudin proposed to use fully saturated edges (by hydrogenation or fluorination) to convert the open-shell singlet narrow CNGs to closed-shell states.[55] Our above computations show that partial hydrogenation can realize the same aim.

Conclusion

The length of zigzag edge determines both kinetic and thermodynamic stabilities of CNGs. CNGs with a long zigzag edge have a small energy gap, whose open-shell singlets and triplets are lower in energy than the closed-shell singlets and are higher in energy than their structural isomers with a long

armchair edge. As a result, among the computationally economic single-determinant wave function methods, using a UBS ansatz is important to properly calculate the ground-state properties for a large CNG. In contrast, the HOMO−LUMO energy gaps of BNNGs have a weak dependence with size; all BNNGs considered here have closed-shell singlet ground states with HOMO−LUMO gaps larger than 5.8 eV. BNNGs with a long zigzag edge have slightly larger kinetic and thermodynamic stabilities than their structural isomers with a long armchair edge, while CNGs have the opposite preference. Chemical modifications that change the long zigzag edge into armchair type can efficiently stabilize the kinetically unstable CNGs (with open-shell singlet ground states) and modify their energy gaps.

Note Added in Proof. During the proof correction period, a paper by Park and Louie[56] reporting first-principles studies on the band gaps of boron nitride nanoribbins appeared on the web.

Acknowledgment. This work was supported in Japan by the Grant-in-Aid for Scientific Research on Priority Area and Next Generation Super Computing Project (Nanoscience Program) from the MEXT of Japan and in the U.S.A. by NSF Grant CHE-0716718 and the Institute for Functional Nanomaterials (NSF Grant 0701525).

Supporting Information Available: Energy differences of the E_{cs} and E_{os} of CNGs and the values of $<S^2>$ of the OSs (Table S1), relative stabilities of isomeric CNGs and BNNGs (Tables S2 and S3), charge distribution of BNNG [6,6] (Figure S1), and full citation of ref 35. This material is available free of charge via the Internet at http://pubs.acs.org.

References and Notes

(1) Geim, A. K.; Novoselov, K. S. *Nat. Mater.* **2007**, *6*, 183.
(2) For a recent reviews see Fukui, K.-i.; Kobayashi, Y.; Enoki, T. *Int. Rev. Phys. Chem* **2007**, *26*, 609.
(3) Jiang, D. E.; Sumpter, B. G.; Dai, S. *J. Chem. Phys.* **2007**, *127*, 124703.
(4) Kobayashi, K. *Phys. Rev. B* **1993**, *48*, 1757.
(5) Klein, D. J. *Chem. Phys. Lett.* **1994**, *217*, 261.
(6) Fujita, M.; Wakabayashi, K.; Nakada, K.; Kusakabe, K. *J. Phys. Soc. Jpn.* **1996**, *65*, 1920.
(7) Nakada, K.; Fujita, M.; Dresselhaus, G.; Dresselhaus, M. S. *Phys. Rev. B* **1996**, *54*, 17954.
(8) Kobayashi, Y.; Fukui, K.-i.; Enoki, T.; Kusakabe, K.; Kaburagi, Y. *Phys. Rev. B* **2005**, *71*, 193406.
(9) Niimi, Y.; Matsui, T.; Kambara, H.; Tagami, K.; Tsukada, M.; Fukuyama, H. *Phys. Rev. B* **2006**, *73*, 085421.
(10) Kan, E. J.; Li, Z.; Yang, J.; Hou, J. G. *J. Am. Chem. Soc.* **2008**, *130*, 4224.
(11) Gusynin, V. P.; Sharapov, S. G. *Phys. Rev. Lett.* **2005**, *95*, 146801.
(12) Novoselov, K. S.; Jiang, Z.; Zhang, Y.; Morozov, S. V.; Stormer, H. L.; Zeitler, U.; Maan, J. C.; Boebinger, G. S.; Kim, P.; Geim, A. K. *Science* **2007**, *315*, 1379.
(13) Abanin, D. A.; Levitov, L. S. *Science* **2007**, *317*, 641.
(14) Williams, J. R.; DiCarlo, L.; Marcus, C. M. *Science* **2007**, *317*, 638.
(15) Zhang, Y.; Tan, Y.-W.; Stormer, H. L.; Kim, P. *Nature* **2005**, *438*, 201.
(16) Novoselov, K. S.; McCann, E.; Morozov, S. V.; Fal'ko, V. I.; Katsnelson, M. I.; Zeitler, U.; Jiang, D.; Schedin, F.; Geim, A. K. *Nat. Phys.* **2006**, *2*, 177.
(17) Novoselov, K. S.; Geim, A. K.; Morozov, S. V.; Jiang, D.; Katsnelson, M. I.; Grigorieva, I. V.; Dubonos, S. V.; Firsov, A. A. *Nature* **2005**, *438*, 197.
(18) Zhou, S. Y. G., G. H.; Graf, J.; Fedorov, A. V.; Spataru, C. D.;.; Diehl, R. D. K., Y.; Lee, D. H.; Louie, S. G.; Lanzara, A. *Nat. Phys* **2006**, *2*, 595.
(19) Novoselov, K. S.; Geim, A. K.; Morozov, S. V.; Jiang, D.; Zhang, Y.; Dubonos, S. V.; Grigorieva, I. V.; Firsov, A. A. *Science* **2004**, *306*, 666.
(20) Stankovich, S.; Dikin, D. A.; Dommett, G. H. B.; Kohlhaas, K. M.; Zimney, E. J.; Stach, E. A.; Piner, R. D.; Nguyen, S. T.; Ruoff, R. S. *Nature* **2006**, *442*, 282.
(21) Liang, X.; Fu, Z.; Chou, S. Y. *Nano Lett.* **2007**, *7*, 3608.
(22) Obradovic, B.; Kotlyar, R.; Heinz, F.; Matagne, P.; Rakshit, T.; Giles, M. D.; Stettler, M. A.; Nikonov, D. E. *Appl. Phys. Lett.* **2006**, *88*, 142102.
(23) Li, X. L.; Wang, X. R.; Zhang, L.; Lee, S.; Dai, H. J. *Science* **2008**, *319*, 1229.
(24) Schedin, F.; Geim, A. K.; Morozov, S. V.; Hill, E. W.; Blake, P.; Katsnelson, M. I.; Novoselov, K. S. *Nat. Mater.* **2007**, *6*, 652.
(25) Zhou, S. Y.; Gweon, G.-H.; Fedorov, A. V.; First, P. N.; de Heer, W. A.; Lee, D.-H.; Guinea, F.; Castro Neto, A. H.; Lanzara, A. *Nat. Mater.* **2007**, *6*, 770.
(26) Zhou, S. Y.; Gweon, G.-H.; Fedorov, A. V.; First, P. N.; de Heer, W. A.; Lee, D.-H.; Guinea, F.; Castro Neto, A. H.; Lanzara, A. *Nat. Mater.* **2007**, *6*, 916.
(27) Han, M. Y.; Özyilmaz, B.; Zhang, Y.; Kim, P. *Phys. Rev. Lett.* **2007**, *98*, 206805.
(28) OKada, S. *Phys. Rev. B* **2008**, *77*, 041408.
(29) Jiang, D. E.; Sumpter, B. G.; Dai, S. *J. Chem. Phys.* **2007**, *126*, 134701.
(30) (a) Bendikov, M.; Duong, H. M.; Starkey, K.; Houk, K. N.; Carter, E. A.; Wudl, F. *J. Am. Chem. Soc.* **2004**, *126*, 7416–7417. (b) Bendikov, M.; Duong, H. M.; Starkey, K.; Houk, K. N.; Carter, E. A.; Wudl, F. *J. Am. Chem. Soc.* **2004**, *126*, 10493.
(31) Hachmann, J.; Dorando, J. J.; Avilés, M.; Chan, G. K. L. *J. Chem. Phys.* **2007**, *127*, 134309.
(32) Jiang, D. E.; Dai, S. *J. Phys. Chem. A* **2008**, *112*, 332.
(33) Novoselov, K. S.; Jiang, D.; Schedin, F.; Booth, T. J.; Khotkevich, V. V.; Morozov, S. V.; Geim, A. K. *Proc. Natl. Acad. Sci. U.S.A.* **2005**, *102*, 10451.
(34) Du, A. J.; Smith, S. C.; Lu, G. Q. *Chem. Phys. Lett.* **2007**, *447*, 181.
(35) Frisch, M. J. et al. *Gaussian 03*, revision C.01; Gaussian, Inc.: Wallingford, CT, 2004.
(36) Houk, K. N.; Lee, P. S.; Nendel, M. *J. Org. Chem.* **2001**, *66*, 5517.
(37) dos Santos, M. C. *Phys. Rev. B* **2006**, *74*, 045426.
(38) Tyutyulkov, N.; Madjarova, G.; Dietz, F.; Müllen, K. *J. Phys. Chem. B* **1998**, *102*, 10183.
(39) Dietz, F.; Tyutyulkov, N.; Madjarova, G.; Müllen, K. *J. Phys. Chem. B* **2000**, *104*, 1746.
(40) Lowdin, P. O. *Phys. Rev.* **1955**, *97*, 1509.
(41) Moran, D.; Stahl, F.; Bettinger, H. F.; Schaefer III, H. F.; Schleyer, P. v. R. *J. Am. Chem. Soc.* **2003**, *125*, 6746.
(42) Stein, S. E.; Brown, R. L. *Carbon* **1985**, *23*, 105.
(43) Stein, S. E.; Brown, R. L. *J. Am. Chem. Soc.* **1987**, *109*, 3721.
(44) Hess, B. A., Jr.; Schaad, L. J. *J. Am. Chem. Soc.* **1971**, *93*, 2413.
(45) Ma, H.; Gao, Y.; Li, X.; Ma, J.; Liu, C.; Jiang, Y. *Internet Electron. J. Mol. Des.* **2003**, *2*, 209–223.
(46) Dias, J. R. *J. Chem. Inf. Model* **2005**, *45*, 562.
(47) Chen, Z. F.; Jiang, D.; Lu, X.; Bettinger, H. F.; Dai, S.; Schleyer, P. v. R.; Houk, K. N. *Org. Lett.* **2007**, *9*, 5449.
(48) Kawai, T.; Miyamoto, Y.; Sugino, O.; Koga, Y. *Phys. Rev. B* **2000**, *62*, R16349.
(49) Radovic, L. R.; Bockrath, B. *J. Am. Chem. Soc.* **2005**, *127*, 5917.
(50) Blasé, X.; Rubio, A.; Louie, S. G.; Cohen, M. L. *Europhys. Lett.* **1994**, *28*, 355.
(51) Blasé, X.; Rubio, A.; Louie, S. G.; Cohen, M. L. *Phys. Rev. B* **1994**, *51*, 6868.
(52) Son, Y.-W.; Cohen, M. L.; Louie, S. G. *Nature* **2006**, *444*, 347–349.
(53) Nendel, M.; Goldfuss, B.; Houk, K. N.; Hafner, K. *J. Mol. Struct. (Theochem)* **1999**, *23*, 461–462.
(54) Sutton, A. P. *Electronic Structure of Materials*; Oxford University Press Inc.: New York, 1996.
(55) Kudin, K. N. *ACS Nano* **2008**, *2*, 516.
(56) Park, C. H.; Louie, S. G. Nano Lett. [Online early access]. DOI: 10.1021/nl080695i. Published Online: July 2, 2008.

JP801679J